www.setjournal.com

Thermo-Mechanical Assessment of Bio-based Insulating Material Using Phase Change Materials and Date Palm Fibers

Mahi Eddine Brahimi¹, Mustapha Maliki¹, Nadia Laredj¹, Hanifi Missoum¹, Miloud Sardou¹

¹Laboratory of Construction, Transport and Environmental Protection LCTPE, University Abdelhamid Ibn Badis of Mostaganem 27000, Algeria.

Abstract

To mitigate extreme temperature fluctuations in arid southern Algerian cities, developing an internal thermal environment that is either independent of or only marginally influenced by external conditions is a viable solution. In this study, we successfully created a eutectic mixture of animal and plant fatty acids, excluding petroleum sources, consisting of 70% myristic acid (MA) and 30% stearic acid (SA). This phase change material (PCM) was then impregnated into date palm fiber waste (DPF) using a vacuum technique. The melting points of both the eutectic mixture and the impregnated date palm fiber were measured at 35°C and 34.5°C, respectively. Clay bricks, which are widely used in Algerian construction, were prepared with 75% dune sand and 10% lime. Date palm fibers impregnated with PCM were added in varying proportions (0.5%, 1%, 1.5%, 2%) to test the mechanical and thermal properties of the bricks. The results showed an improvement in thermal insulation, with a reduction in thermal conductivity by 11% for bricks containing 2% impregnated palm fibers. The compressive strength of these bricks remained within acceptable limits, regardless of whether the PCM was in a solid or liquid state. Numerical simulations showed that adding MA-SA/DPF to clay bricks contributed to a 30% reduction in outward heat flow in winter and a 25% reduction in inward heat flow in summer. This, in turn, resulted in a corresponding decrease in energy consumption.

Keywords: Phase change materials, Brick, Thermal conductivity, Date palm fiber, compressive strength.

1. Introduction

Using local renewable resources for building materials is essential for the construction industry. Over one-third of total energy consumption and half of global electricity usage occur within this sector. Consequently, the building industry is responsible for significant carbon dioxide emissions worldwide. CO₂ is a valuable metric for assessing the carbon footprint of various building materials and methods. Earth buildings often produce fewer CO₂ emissions than traditional construction methods due to the lower energy required for their production and transport, as well as the use of low-carbon materials. As a result, earthen construction techniques can significantly reduce building-related emissions [1].

Various types of earthen bricks are commonly used, particularly adobe, which is favored in construction due to its cost-effectiveness and the accessibility of its raw materials. Research indicates that adobe bricks can be made from locally sourced materials, such as dune sand and crushed brick waste, which enhance their mechanical properties and thermal efficiency while reducing environmental impact [2]. Over the years, many additives have been introduced to improve the mechanical and physical properties of adobe. However, earthen bricks tend to have weak resistance, which is why cement or lime is often added to strengthen them [3]. Improving the compressive strength of adobe results in stronger walls, higher-quality buildings, and more durable structures [4]. Observations indicate that existing adobe buildings

typically have a compressive strength ranging from 0.2 to 2 MPa [5]. Many research studies have focused on improving thermal insulation and selecting suitable materials for walls to reduce the energy consumed by heating and air conditioning systems [6], [7], [8]. Various waste materials have been incorporated into earthen bricks without compromising their essential properties [9] such as date palm fibers [10], [11]. In this context, researchers have shown great interest in enhancing the thermal properties of wall components. Phase change materials (PCMs) have been a focal point in this area due to their ability to absorb heat during melting and release it upon solidification when the temperature drops below the freezing point of the PCM [12]. PCMs can be categorized into organic and inorganic types. Organic PCMs are further divided into paraffinic and non-paraffinic materials [13]. While paraffin is petroleum-based, nonparaffinic materials like fatty acids and fatty alcohols are renewable and do not rely on fossil fuels. These renewable materials offer several benefits, including strong thermal and chemical stability, a high capacity for storing latent heat, appropriate phase transition temperatures, and the absence of issues like supercooling or phase separation [14]. Additionally, they are cost-effective and noncorrosive [15]. However, due to the high cost of petroleum-based PCMs, fatty acids have attracted considerable attention because of their availability, low cost, and plant or animal origins [16]. Fatty acids and fatty alcohols generally have phase transition temperatures that are higher than ideal, limiting their use to specific applications such as residential heating and building construction. To overcome this limitation, a stable eutectic mixture can be created by melting and mixing two or more fatty acids and their components, allowing for a more suitable temperature range [17]. To reduce energy consumption in building envelopes, the development and use of efficient energy storage technologies are becoming increasingly important. PCM-based thermal energy storage is a particularly attractive method for storing and utilizing solar energy on demand in buildings [18].

The purpose of this study is to improve the energy efficiency of buildings by using environmentally friendly materials. Date palm fibers (DPF) and phase change materials (PCM) were combined in clay bricks. Initially, a eutectic mixture of fatty acids, sourced from the Algerian market, was prepared and successfully infused into date palm fibers. This new compound was then

incorporated into clay bricks. The resulting bricks were subjected to mechanical, physical, and thermal testing to evaluate their properties. Additionally, a numerical simulation was conducted to quantify heat flux reduction when using DPF/PCM in clay building walls.

2. Materials and methods

2.1. Traditional building materials (Soil, sand and lime)

This research aims to utilize local resources such as soil, sand, and palm fibers from the cities of Adrar and Ouargla, located in the southwest and southeast of Algeria, respectively. These regions are renowned for their high temperatures, which can exceed 55°C.

2.1.1. Clay soil

The clay was assessed based on its chemical composition, with a focus on key oxides such as SiO₂, Al₂O₃, and Fe₂O₃, while the presence of CO₂ and CaCO₃ was found to be minimal (Table 1). From an industrial perspective, the Al₂O₃/Fe₂O₃ ratio is less than 5.5, indicating a high iron content, which makes this clay suitable for producing building materials such as bricks and tiles [19]. This soil has been used in many studies [20], [21], [22].

2.1.2. Dune Sand and lime

Dune sand from the Adrar region of Algeria was used in the production of all brick mixes. The chemical composition of this sand and soil is provided in Table 1. Quicklime from the lime unit in Saïda, Algeria, was also utilized.

2.2. Date palm fibers

Date palm natural fibers (DPF) were obtained from Touggourt Oasis and had an absolute density of $1300 \div 1450 \text{ Kg m}^{-3}$, length L = $10 \pm 1 \text{ mm}$, diameter $\phi = 0.14 \div 1.7 \text{ mm}$, the tensile strength and moisture content in the range of $170 \div 290 \text{ MPa}$ and $9.5 \div 10.5 \%$, respectively [23]. The density of $610 \pm 40 \text{ kg m}^{-3}$ falls within the same range as that determined for date palm (Phoenix dactylifera L.) from the Biskra Oasis in Algeria.

Component (%) SiO₃ CaO Al₂O₃ FeO₃ CaCO₃ CO_2 Soil 82.10 1.96 3.33 4.41 0.93 0.41 Sand 87.1 6.3 0.01 1.35 4.55 2.03

Table 1. Chemical properties of the soil and dune sand used in the present study.

Table 2. Properties of the organic PCMs.

Phase change material	Melting Temperature (°C)	Latent heat (J/g)	Price (\$/kg)
Myristic acid (C ₁₄ H ₂₈ O ₂)	54	210	6.6
Stearic acid (C ₁₈ H ₃₆ O ₂)	68	258	6.6

2.3. Fatty Acids properties

Myristic acid (MA, C₁₄H₂₈O₂, analytical reagent) and stearic acid (SA, C₁₈H₃₆O₂, analytical reagent) were purchased from Merck. Myristic acid has a melting temperature of 54°C, while stearic acid melts at 68°C. Both acids are available in Algeria. The MA-SA eutectic mixture was formulated following the experimental procedure described by Homlakorn et al. [24]. The eutectic mixture (MA-SA: 70–30 wt%) melts at 35°C with a latent heat of 240 J/g and solidifies at 35.5°C with a latent heat of 212 J/g. Its density is 0.84 g/cm³ in the liquid state and 0.74 g/cm³ in the solid state. The properties of both acids are listed in Table 2.

2.4. Experimental setup

2.4.1. Preparation and characterization of shapestabilized phase change material (SS-PCM)

The SS-PCM composites were produced using the vacuum impregnation method, which enhances phase change material (PCM) absorption into the support's pores by eliminating trapped air [25]. The experimental steps for creating the shape-stabilized eutectic mixture (70% myristic acid (MA) and 30% stearic acid (SA)) were as follows: A specific mass ratio of myristic acid to stearic acid was mixed in a test tube. The test tube was then heated in a constant-temperature water bath at 80°C and stirred with a magnetic stirrer at 400 revolutions per minute for 1 hour to ensure homogeneity. Figure 1 summarizes the preparation process.

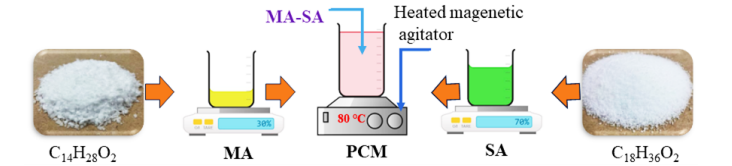


Figure 1. The method used for preparing the eutectic mixture MA-SA.

2.4.2. Preparation of MA-SA/DPF composites

To obtain the MA-SA/DPF stable-form composite, the vacuum impregnation technique was used (Figure 2). Date palm fiber was weighed (m₁) and mixed with the preweighed liquid MA-SA. Both the date palm fibers and the eutectic mixture were placed in a conical flask, which was then placed in a water bath at 60°C, a temperature higher than the melting point of the PCM. Next, a vacuum pump was connected and activated to evacuate air from the porous structure of the DPF.

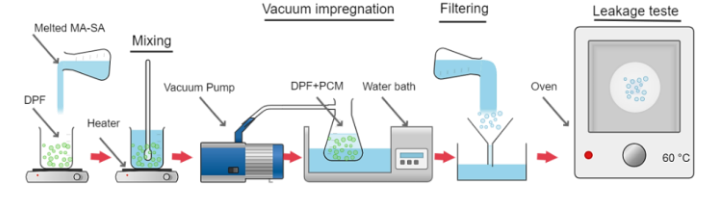


Figure 2. Fabrication process of the DPF/MA-SA by vacuum impregnation method.

The vacuum process was maintained for 1 hour to ensure complete impregnation. The melted MA-SA was absorbed into the pores of the date palm fiber by capillarity and surface tension forces [26].

Date palm Biochar Wood flour Wood fibers Kapok fibers Hemp shives fiber **Impregnation** 48.5 44 52 40.5 53 52.39 (%)Reference [29] [30] This study [27] [28] [31]

Table 1. Comparison between the Percentage of impregnation of the prepared MA-SA/ DPF composite with that of other biobased PCM composites.

After impregnation, the vacuum process was terminated, and the samples were removed. Any excess liquid MA-SA was filtered out. The impregnated date palm fiber was then placed on filter paper and kept in an oven at 60°C to remove any remaining MA-SA on the fiber surface. The filter paper was continuously replaced until no leakage was observed. Finally, the final mass of the composite (m₂) was weighed, and the mass ratio of MA-SA in the composite was calculated using Equation (1), as described in [26].

$$R = \frac{m_2 - m_1}{m_2} \times 100 \tag{1}$$

The final mass ratio without leakage was 52.39%. This value is comparable to the values reported in the literature for fibers, as shown in Table 3.

2.4.3 Preparation of samples

The optimal dune sand content for compressive strength was determined to be 75% by weight, as shown in Figure 3. A water content of 25% by weight was selected to achieve a uniform mixture suitable for molding adobes. Mixing was performed using an electric mixer for 15 minutes to ensure homogeneity. The mixtures were manually filled into cubic molds ($10 \times 10 \times 10$ cm) in two layers and left to dry in the open air for 72 hours. Afterward, the blocks were removed from the molds and air-cured. The lime content was optimized for compressive strength. After that, the appropriate amount of water, relative to the total mass, was added to transform the mixture from a damp blend into a uniform paste ready for molding [32]. Various lime contents (4%, 6%, 8%, 10%, 12%, and 14% by weight) were tested, with 10% being the optimal value, as shown in Figure 4.

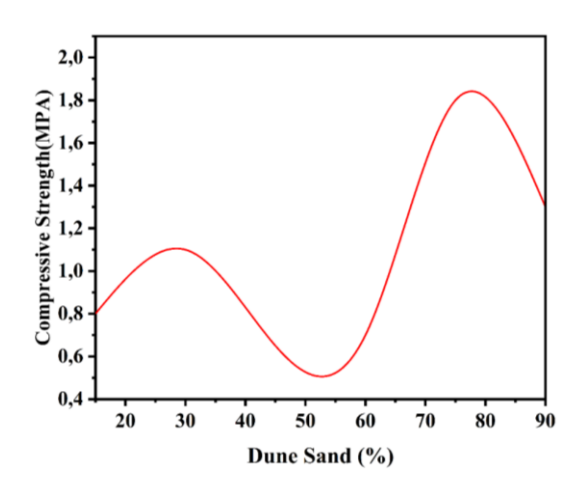


Figure 3. Effect of dune sand percentage on dry compressive strength of clay.

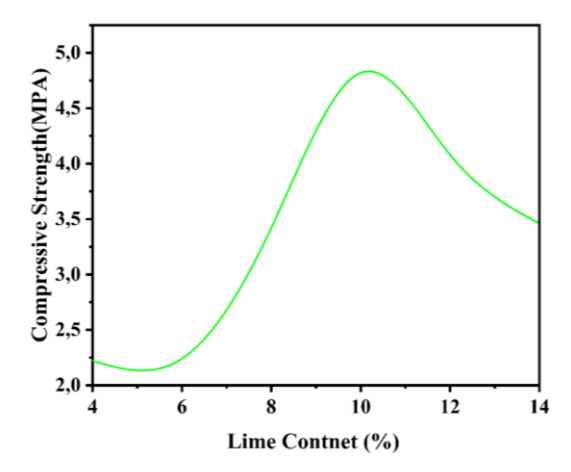


Figure 4. Effect of lime percentage on dry compressive strength of clay.

After optimizing the lime content, bricks were manufactured using a mixture of soil, sand, lime, and MA-SA/DPF. The mixing and preparation process was conducted in two stages. First, the dry mixture (soil + sand + lime) was mixed for 5 minutes. Then, water was added, and the mixture was further mixed for 15 minutes until homogenization. Finally, the required quantity of MA-SA/DPF was gradually added while continuing manual mixing.

Mixture	Dune Sand (%)	Soil (%)	Lime (relative to the weight of sand + Soil)	MA-SA/DPF	
1	75	25	10	0	
2	75	25	10	0,5	
3	75	25	10	1	
4	75	25	10	1,5	
	75	25	10	2	

Table 2. Percentage of building materials in various prepared mixtures.

The proportions of the different mixtures are presented in Table 4. It is worth noting that the cubic $(10 \times 10 \times 10 \text{ cm})$ and prismatic $(4 \times 4 \times 16 \text{ cm})$ metal molds were filled in two layers, and three test pieces were prepared for each test, as shown in Figure 5.



Figure 5. Compressive strength test specimens with various dimensions.

3. Thermo-Mechanical Analysis

3.1. Mechanical characterization

According to French norm NF-EN 196-1, the dry compressive strength was determined on cubic blocks measuring (10 x 10 x 10) cm using a hydraulic press as shown in figure 5. Employing a force sensor of 20 kN with a loading speed of 0.5 mm/min, this enabled the construction of compressive and flexural stress-strain diagrams, facilitating the observation of the material's mechanical response under dry compression and bending at various DPF contents for both natural and PCM states (solid and liquid). Each composition was tested using a three-point test configuration. The two prism halves from this test were used for compression testing.

3.2. Characterization of DPF/MA-SA composites

3.2.1. Differential Scanning Calorimetry (DSC)

Differential Scanning Calorimetry (DSC) was used to assess the thermal energy storage capability by examining the melting characteristics of the prepared PCM composite. Figure 6 displays the DSC curve representing the eutectic MA-SA and DPF/MA-SA composite.

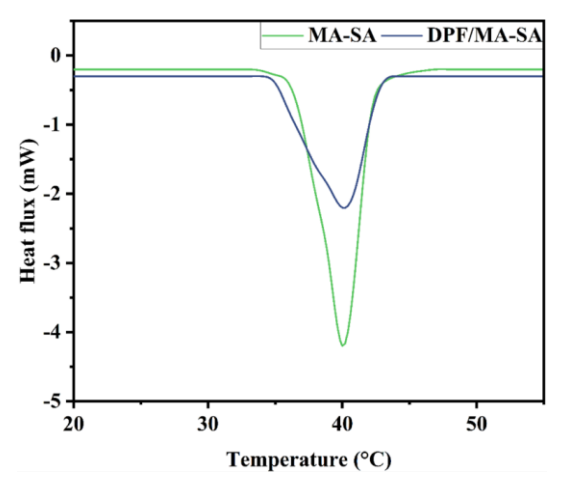


Figure 6. DSC curve of MA-SA, PCM only and DPF/MA-SA composite.

The melting temperatures for MA-SA and DPF/MA-SA composite were identified as 35 °C and 34.5 °C, respectively. The melting enthalpies were 240 J/g and 124 J/g, respectively. After fabricating the shape-stabilized DPF/MA-SA composite, the melting enthalpy showed a reduction. This decrease is attributed to:

- 1. The lower mass ratio of eutectic MA-SA within the composite.
 - 2. The reduced crystallinity of eutectic MA-SA.

Furthermore, the phase change temperature of the composite PCM was slightly lower than that of pure eutectic MA-SA before impregnation. This shift may be due to weak attractive interactions between fatty acid molecules and the inner surface of the porous material

[33]. The measured melting and solidifying temperatures of the composite PCM closely match the values calculated by multiplying the eutectic MA-SA ratio in the composite by its phase transition enthalpy, as reported by [34]. In fact, the fusion heat ratio of pure eutectic MA-SA and DPF/MA-SA is 51.66%, which is remarkably close to the theoretical impregnation rate of 52.39%.

3.2.2 Thermo-Gravimetric Analysis (TGA)

Figure 7 illustrates the weight loss curves for MA-SA, DPF alone, and the DPF/MA-SA composite from room temperature (25°C) to 350°C. The curves indicate that MA-SA primarily degrades between 125°C and 180°C. For DPF alone, the TGA curve shows an initial weight loss between 75°C and 175°C, attributed to the evaporation of free water in the DPF. The MA-SA/DPF composite demonstrates good thermal stability below 125°C, with less than 1% mass loss, making it suitable for building applications where temperatures rarely exceed 60°C.

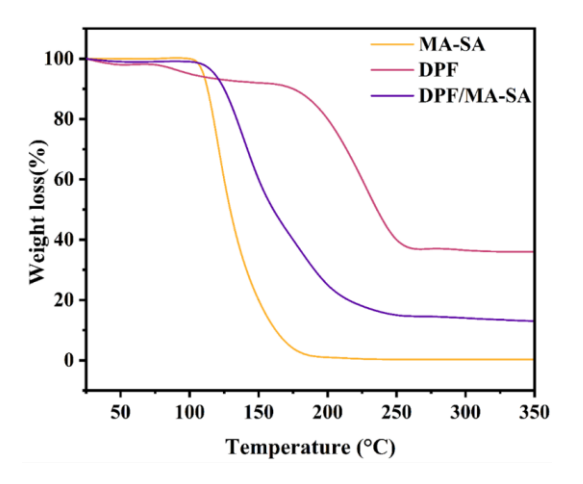


Figure 7. TGA curve of MA-SA, DPF only and MA-SA/DPF.

4. Results and Discussions

4.1. Effect of DPF/MA-SA content ratio on the physical properties of Earth bloc

4.1.1 Apparent density

The density of adobe, as reported in the literature, ranges from 1540 kg/m³ to 1950 kg/m³ [35]. In this study, the apparent density of dried specimens was determined by comparing the weight of the soil block to its volume. Figure 8 presents the average density values of the

formulated material for different DPF/MA-SA contents, ranging from 1542 kg/m³ to 1608 kg/m³.

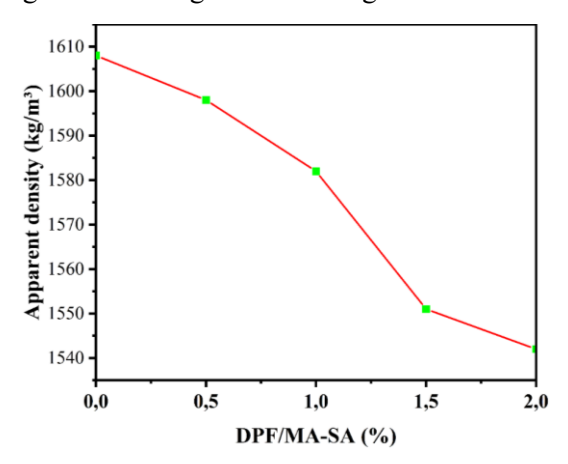


Figure 1. Variation of the apparent density as a function of the percentage of MA-SA/DPF.

A notable density reduction of 606 kg/m³ was observed for the 2% DPF/MA-SA content compared to the control material (without DPF/MA-SA). This reduction is attributed to:

- 1. The lower apparent density of date palm fiber and the MA-SA mixture (840 kg/m 3) compared to the adobe mixture (soil + dune sand + lime = adobe), which has an apparent density of 1608 kg/m 3 .
- 2. The evaporation of water, which led to the detachment of DPF/MA-SA particles from the clay matrix after shrinkage, increasing the porous network within the material.

Similar trends have been reported in previous studies [35].

4.1.2 Total absorption

Figure 9 illustrates the relationship between total water absorption of bricks and DPF/MA-SA content over a 24-hour immersion period at two temperature conditions, 30°C and 50°C. At temperatures below 30°C, total water absorption ranged from 18.22% for 0% DPF/MA-SA to 18.56% for 2% DPF/MA-SA. This increase is minimal compared to previous studies using date palm fibers, likely due to pore closure caused by the eutectic mixture. The slight rise in absorption is attributed to DPF/MA-SA disintegration within the matrix composed of soil, dune sand, and lime. At 50°C, the absorption rate increased to 18.95% for 2% DPF/MA-SA. This increase is due to the eutectic mixture transitioning to a liquid state, allowing

water infiltration into newly formed pores. Additionally, total water absorption increased with higher DPF/MA-SA content. Despite this, adding DPF/MA-SA does not significantly increase total water absorption. After six days of immersion, the blocks retained their original shape and integrity, demonstrating excellent stability, which is a notable advantage for earthen construction.

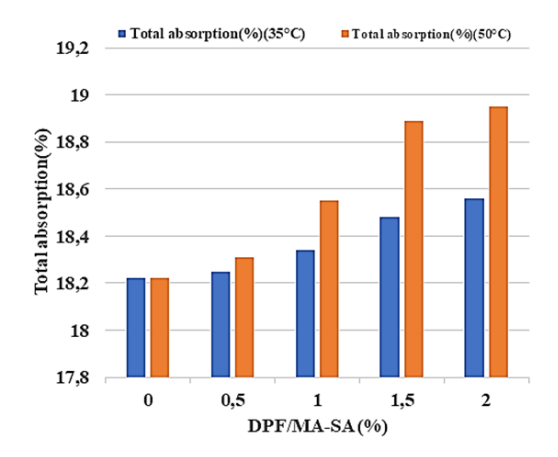


Figure 9. Effect of MA-SA/DPF on total absorption of bricks.

4.2. Effect of MA-SA/DPF content on the thermomechanical properties of adobes

4.2.1 Compressive strength

This study examined the effect of varying DPF/MA-SA content on the compressive strength of bricks at different temperatures. The tests were conducted on 10×10×10 cm³ bricks at 30°C and 50°C. As shown in Figure 10, increasing the DPF/MA-SA content reduced bulk density and slightly decreased compressive strength. The highest compressive strength was observed in control bricks without DPF/MA-SA, averaging 4.8 MPa. Even at a 2% DPF/MA-SA content, the reduction in strength was minimal and not considered significant. At approximately 0.5% DPF/MA-SA, the compressive strength remained similar to that of bricks without DPF/MA-SA. Contrary to previous studies, the addition of DPF to earthen bricks did not significantly weaken them. This was attributed to the treatment of fibers with MA-SA, which closed the pores when in a solid state. However, when the bricks were exposed to 50°C for two hours, ensuring that the MA-SA mixture transitioned into a liquid state, the compressive strength decreased compared to the first case. The liquid MA-SA mixture opened the pores, reducing overall strength.

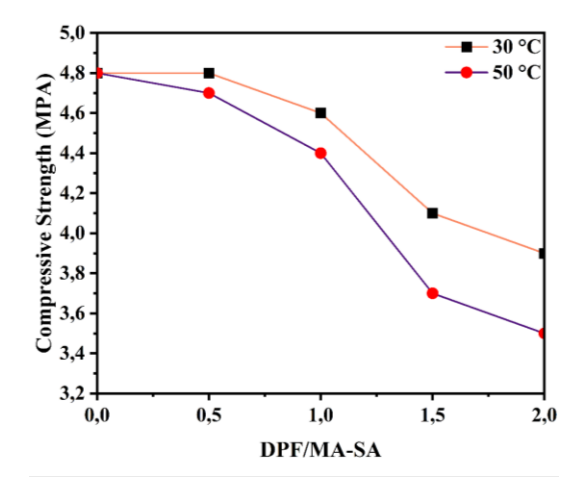


Figure 2. Effect of MA-SA/DPF content on the dry compressive strength of adobe.

Despite this, the lowest recorded compressive strength values in both cases remained within the acceptable limits for building requirements in Algeria [36]. The decrease in strength was linked to the increase in voids within the blocks due to the separation of DPF/MA-SA aggregates from the stabilized ground matrix in dry bricks and the separation of MA-SA from DPF in the liquid state. The dry compressive strength of earthen bricks primarily depends on the strength of the binder, the bond strength of clay putty stabilized with lime sand grains, and the internal strength of the sand particles [37].

4.2.2 Thermal Conductivity

Thermal conductivity was evaluated on brick samples measuring 10×10×4 cm. The measurements were performed using a hot wire probe and a heating resistor, accompanied by a sensor that recorded temperature variations in a transient state. To ensure precision, the probe was placed between two smooth blocks to eliminate air gaps. This method is widely adopted in various research studies [38]. All measurements were conducted at an ambient laboratory temperature of 24°C with 60% humidity, and the results were consistent with findings from other researchers [35], [39]. As shown in Figure 11, thermal conductivity decreases as the DPF/MA-SA content increases, leading to an 11% improvement in thermal insulation. Adobe containing 2% DPF/MA-SA exhibited a thermal conductivity of 0.554 W/m·K, compared to 0.677 W/m·K for control adobe. This enhancement in thermal performance is attributed to the improved pore structure of bricks incorporating DPF/MA-SA [40].

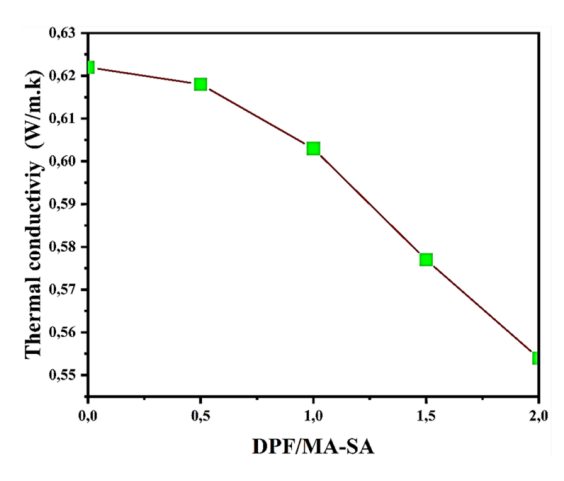


Figure 3. Effect of MA-SA/DPF ratio on thermal conductivity.

This reduction is due to the lower density of MA-SA/DPF compared to the clay matrix and its inherently low thermal conductivity. The difference in thermal conductivity between the clay matrix and date palm aggregates primarily results from variations in pore sizes and the volume of PCM, which has a very low thermal conductivity (0.17 W/m·K). These findings align with those reported by other researchers [41]. Additionally, the thermal conductivity values obtained comply with the Algerian building code, which specifies a range between 0.1 and 2 W/m·K [42].

4.3. Numerical modeling of the DPF/MA-SA product effectiveness

To evaluate the performance of the proposed bricks, heat flow variations in two walls were simulated using the COMSOL Multiphysics program—one wall with a DPF/MA-SA mixture and the other without. The simulations were performed for both a summer and a winter day, with boundary conditions derived from local climate data (Algeria). For the outer surface, external convective boundary conditions were applied with a heat transfer coefficient of $h_0 = 25 \text{ W/m}^2 \cdot \text{K}$. On the inner surface, a free convective boundary condition was used with $h_i = 6.69 \text{ W/m}^2 \cdot \text{K}$ [43]. The results demonstrated the effectiveness of the brick, as shown in Figure 12. Numerical simulations show that adding MA-SA/DPF to clayey bricks contributes to a 30% reduction in outward heat flow during winter and a 25% reduction in inward heat flow during summer.

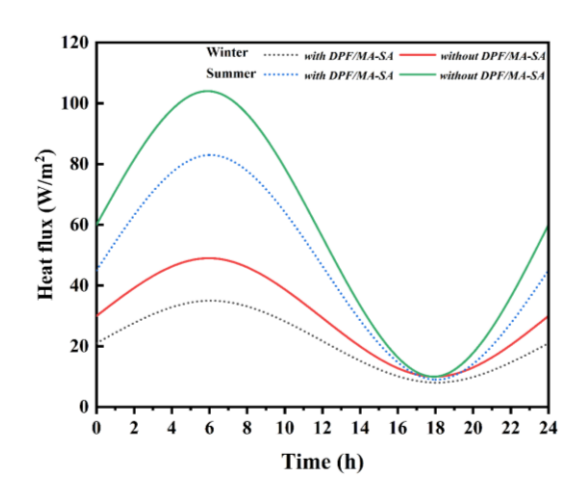


Figure 12. Effect of MA-SA/DPF addition on heat flow reduction.

5. Conclusion

This study innovatively investigated the impact of a new eutectic mixture of fatty acids combined with date palm fibers on lime-stabilized soil. It specifically analyzed the thermal properties and mechanical behavior of the material in both solid and liquid states across a temperature range varying from 30°C to 50°C. The research also examined the effect of different amounts of date palm fibers on these properties. The results indicated that the soil achieved its maximum dry compressive strength when the quicklime content was 10% by weight.

For the first time, the MA-SA eutectic mixture was successfully combined with waste date palm fibers (DPF) from the Algerian Sahara, creating a low-cost and environmentally friendly phase change material (PCM) suitable for integration with earthen bricks. The eutectic mixture, consisting of 70% myristic acid and 30% stearic acid, was successfully prepared, achieving a melting point of 35°C and maintaining stability at temperatures below 85°C, as confirmed by DSC and TGA analyses.

The MA-SA mixture was effectively infused into date palm fibers, achieving an incorporation rate of 52.39%. DSC analysis revealed that the MA-SA/DPF composite exhibits promising melting properties, with a melting temperature of 34.5°C and a measured melting enthalpy of 124 J/g. Although the composite has a lower latent heat compared to pure PCM, these results remain highly promising for energy storage applications in buildings.

The newly developed clay bricks, reinforced with palm fiber residues and infused with a phase change material derived from animal and plant sources (non-petroleum), successfully met the mechanical standards required by Algerian building codes. Additionally, these bricks demonstrated significant thermal improvements, making them an excellent eco-friendly alternative for construction. By utilizing abundant and free resources, they contribute to environmental sustainability.

Conflicts Interest Statement

The authors declare that they have no known competing financial interests or personal relationships that could have appeared to influence the work reported in this paper.

Data Availability Statement

Supplementary materials and data used in this research are accessible upon request. For access, please contact the corresponding author via [mustafa.maliki@univmosta.dz].

Author Contribution Roles

Mahi Eddine Brahimi - Conceptualization, Software, Investigation, Writing, Original Draft. Mustapha Maliki - Methodology, Software, Project administration. Nadia Laredj - Methodology, Investigation, Resources. Hanifi Missoum - Conceptualization, Supervision. Miloud Sardou - Supervision.

References

- [1] S. H. Ghaffar, M. Al-Kheetan, P. Ewens, T. Wang, and J. Zhuang, "Investigation of the interfacial bonding between flax/wool twine and various cementitious matrices in mortar composites," *Constr Build Mater*, vol. 239, Apr. 2020, doi: 10.1016/j.conbuildmat.2019.117833.
- [2] A. Sánchez, H. Varum, T. Martins, and J. Fernández, "Mechanical properties of adobe masonry for the rehabilitation of buildings," May 23, 2022, *Elsevier Ltd.* doi: 10.1016/j.conbuildmat.2022.127330.
- [3] H. B. Nagaraj, M. V. Sravan, T. G. Arun, and K. S. Jagadish, "Role of lime with cement in long-term strength of Compressed Stabilized Earth Blocks," *International Journal of Sustainable Built Environment*, vol. 3, no. 1, pp. 54–61, 2014, doi: 10.1016/j.ijsbe.2014.03.001.
- [4] C. Belebchouche, O. Temami, M. L. K. KHOUADJIA, S. Hamlaoui, A. Berkouche, and T. Chouadra, "Recycling of Brick and Road Demolition Waste in the Production of

- Concrete," *Science, Engineering and Technology*, vol. 4, no. 2, pp. 14–23, Sep. 2024, doi: 10.54327/set2024/v4.i2.154.
- [5] F. Fratini, E. Pecchioni, L. Rovero, and U. Tonietti, "The earth in the architecture of the historical centre of Lamezia Terme (Italy): Characterization for restoration," *Appl Clay Sci*, vol. 53, no. 3, pp. 509–516, Sep. 2011, doi: 10.1016/j.clay.2010.11.007.
- [6] A. El bourki, A. Koutous, and E. Hilali, "A review on the use of date palm fibers to reinforce earth-based construction materials," *Mater Today Proc*, Jun. 2023, doi: 10.1016/j.matpr.2023.05.613.
- [7] M. Maliki, N. Laredj, H. Missoum, K. Bendani, and H. Naji, "A coupled heat and mass transfer model for energy saving in building components," in *OPT-i 2014 1st International Conference on Engineering and Applied Sciences Optimization, Proceedings*, 2014.
- [8] M. Maliki, N. Laredj, H. Missoum, K. Bendani, and H. Naji, "Numerical modelling of coupled heat, air and moisture transfer in building envelopes," *Mechanics and Industry*, vol. 16, no. 5, 2015, doi: 10.1051/meca/2015033.
- [9] A. E. Losini, A. C. Grillet, M. Bellotto, M. Woloszyn, and G. Dotelli, "Natural additives and biopolymers for raw earth construction stabilization – a review," Oct. 18, 2021, *Elsevier Ltd.* doi: 10.1016/j.conbuildmat.2021.124507.
- [10] A. Eslami, H. Mohammadi, and H. Mirabi Banadaki, "Palm fiber as a natural reinforcement for improving the properties of traditional adobe bricks," *Constr Build Mater*, vol. 325, Mar. 2022, doi: 10.1016/j.conbuildmat.2022.126808.
- [11] A. El bourki, A. Koutous, and E. Hilali, "A review on the use of date palm fibers to reinforce earth-based construction materials," *Mater Today Proc*, Jun. 2023, doi: 10.1016/j.matpr.2023.05.613.
- [12] G. P. Panayiotou, S. A. Kalogirou, and S. A. Tassou, "Evaluation of the application of Phase Change Materials (PCM) on the envelope of a typical dwelling in the Mediterranean region," *Renew Energy*, vol. 97, pp. 24–32, Nov. 2016, doi: 10.1016/j.renene.2016.05.043.
- [13] P. K. S. Rathore and S. K. Shukla, "Enhanced thermophysical properties of organic PCM through shape stabilization for thermal energy storage in buildings: A state of the art review," Apr. 01, 2021, *Elsevier Ltd.* doi: 10.1016/j.enbuild.2021.110799.
- [14] Y. Yuan, N. Zhang, W. Tao, X. Cao, and Y. He, "Fatty acids as phase change materials: A review," 2014. doi: 10.1016/j.rser.2013.08.107.
- [15] A. Bashiri Rezaie and M. Montazer, "Shape-stable thermo-responsive nano Fe3O4/fatty acids/PET composite phase-change material for thermal energy management and saving applications," *Appl Energy*, vol. 262, Mar. 2020, doi: 10.1016/j.apenergy.2020.114501.
- [16] M. Jafaripour, S. M. Sadrameli, H. Pahlavanzadeh, and S. A. H. S. Mousavi, "Fabrication and optimization of kaolin/stearic acid composite as a form-stable phase change material for application in the thermal energy

- storage systems," *J Energy Storage*, vol. 33, Jan. 2021, doi: 10.1016/j.est.2020.102155.
- [17] M. Sun *et al.*, "A review on thermal energy storage with eutectic phase change materials: Fundamentals and applications," Sep. 15, 2023, *Elsevier Ltd.* doi: 10.1016/j.est.2023.107713.
- [18] E. Oró, A. de Gracia, A. Castell, M. M. Farid, and L. F. Cabeza, "Review on phase change materials (PCMs) for cold thermal energy storage applications," 2012, *Elsevier Ltd.* doi: 10.1016/j.apenergy.2012.03.058.
- [19] M. Garcia-Valles, P. Alfonso, S. Martínez, and N. Roca, "Mineralogical and thermal characterization of kaolinitic clays from terra alta (Catalonia, Spain)," *Minerals*, vol. 10, no. 2, Feb. 2020, doi: 10.3390/min10020142.
- [20] A. Bassoud, H. Khelafi, A. M. Mokhtari, and A. Bada, "Effectivenessof salty sand in improving the adobe's thermomechanical properties: Adrar case study (south Algeria)," *Trends in Sciences*, vol. 18, no. 19, Oct. 2021, doi: 10.48048/tis.2021.6.
- [21] A. Bada, H. Khelafi, and A. Mokhtari, "Etude et Caractérisation Thermomécanique Des Matériaux Locaux A Base D'argile-Argile D'Adrar," International Journal of Scientific Research & Engineering Technology - IJSET Vol.5 pp.5-8, 2017.
- [22] A. Bassoud, H. Khelafi, A. M. Mokhtari, and A. Bada, "Effectivenessof salty sand in improving the adobe's thermomechanical properties: Adrar case study (south Algeria)," *Trends in Sciences*, vol. 18, no. 19, Oct. 2021, doi: 10.48048/tis.2021.6.
- [23] M. L. Bakhaled, M. Bentchikou, R. Belarbi, and M. Maliki, "Elaboration and characterization of extruded clay bricks with light weight date palm fibers," *Materials Testing*, vol. 63, no. 9, pp. 872–877, Sep. 2021, doi: 10.1515/mt-2021-0011.
- [24] S. Homlakorn, A. Suksri, and T. Wongwuttanasatian, "Efficiency improvement of PV module using a binary-organic eutectic phase change material in a finned container," *Energy Reports*, vol. 8, pp. 121–128, Nov. 2022, doi: 10.1016/j.egyr.2022.05.147.
- [25] C. Cárdenas-Ramírez, M. A. Gómez, and F. Jaramillo, "Comprehensive analysis of the thermal properties of capric-myristic, lauric-myristic and palmitic-stearic acids and their shape-stabilization in an inorganic support," *J Energy Storage*, vol. 34, p. 102015, Feb. 2021, doi: 10.1016/J.EST.2020.102015.
- [26] W. Zhang *et al.*, "Lauric-stearic acid eutectic mixture/carbonized biomass waste corn cob composite phase change materials: Preparation and thermal characterization," *Thermochim Acta*, vol. 674, pp. 21–27, Apr. 2019, doi: 10.1016/j.tca.2019.01.022.
- [27] G. Hekimoğlu *et al.*, "Walnut shell derived biocarbon/methyl palmitate as novel composite phase change material with enhanced thermal energy storage properties," *J Energy Storage*, vol. 35, Mar. 2021, doi: 10.1016/j.est.2021.102288.
- [28] X. Jingchen et al., "Form-stable phase change material based on fatty acid/wood flour composite and PVC used

- for thermal energy storage," *Energy Build*, vol. 209, Feb. 2020, doi: 10.1016/j.enbuild.2019.109663.
- [29] A. Sarı, G. Hekimoğlu, and V. V. Tyagi, "Low cost and eco-friendly wood fiber-based composite phase change material: Development, characterization and lab-scale thermoregulation performance for thermal energy storage," *Energy*, vol. 195, Mar. 2020, doi: 10.1016/j.energy.2020.116983.
- [30] T. Dong *et al.*, "A phase change material embedded composite consisting of kapok and hollow PET fibers for dynamic thermal comfort regulation," *Ind Crops Prod*, vol. 158, Dec. 2020, doi: 10.1016/j.indcrop.2020.112945.
- [31] M. Sawadogo, F. Benmahiddine, A. E. A. Hamami, R. Belarbi, A. Godin, and M. Duquesne, "Investigation of a novel bio-based phase change material hemp concrete for passive energy storage in buildings," *Appl Therm Eng*, vol. 212, Jul. 2022, doi: 10.1016/j.applthermaleng.2022.118620.
- [32] Z. Assia, F. Fazia, and H. Abdelmadjid, "Sustainability of the stabilized earth blocs under chemicals attack's effects and environmental conditions," *Constr Build Mater*, vol. 212, pp. 787–798, Jul. 2019, doi: 10.1016/j.conbuildmat.2019.03.324.
- [33] A. Karaipekli and A. Sari, "Preparation, thermal properties and thermal reliability of eutectic mixtures of fatty acids/expanded vermiculite as novel form-stable composites for energy storage," *Journal of Industrial and Engineering Chemistry*, vol. 16, no. 5, pp. 767–773, Sep. 2010, doi: 10.1016/j.jiec.2010.07.003.
- [34] O. Chung, S. G. Jeong, and S. Kim, "Preparation of energy efficient paraffinic PCMs/expanded vermiculite and perlite composites for energy saving in buildings," *Solar Energy Materials and Solar Cells*, vol. 137, pp. 107–112, 2015, doi: 10.1016/j.solmat.2014.11.001.
- [35] D. Khoudja, B. Taallah, O. Izemmouren, S. Aggoun, O. Herihiri, and A. Guettala, "Mechanical and thermophysical properties of raw earth bricks incorporating date palm waste," *Constr Build Mater*, vol. 270, Feb. 2021, doi: 10.1016/j.conbuildmat.2020.121824.
- [36] D. Silveira, H. Varum, A. Costa, T. Martins, H. Pereira, and J. Almeida, "Mechanical properties of adobe bricks in ancient constructions," *Constr Build Mater*, vol. 28, no. 1, pp. 36–44, Mar. 2012, doi: 10.1016/j.conbuildmat.2011.08.046.
- [37] F. Parisi, D. Asprone, L. Fenu, and A. Prota, "Experimental characterization of Italian composite adobe bricks reinforced with straw fibers," *Compos Struct*, vol. 122, pp. 300–307, Apr. 2015, doi: 10.1016/j.compstruct.2014.11.060.
- [38] H. Niroumand, M. F. M. Zain, M. Jamil, and S. Niroumand, "Earth Architecture from Ancient until Today," *Procedia Soc Behav Sci*, vol. 89, pp. 222–225, Oct. 2013, doi: 10.1016/j.sbspro.2013.08.838.
- [39] A. Oushabi, S. Sair, Y. Abboud, O. Tanane, and A. El Bouari, "An experimental investigation on morphological, mechanical and thermal properties of date palm particles reinforced polyurethane composites as new ecological

- insulating materials in building," *Case Studies in Construction Materials*, vol. 7, pp. 128–137, Dec. 2017, doi: 10.1016/j.cscm.2017.06.002.
- [40] G. Matthew, O. Sanya, and N. Mohammed, "Influence of Pore Nature on the Thermal Conductivity of Insulating Refractory Brick," *Chemistry and Materials Research*, Sep. 2020, doi: 10.7176/cmr/12-7-03.
- [41] A. B. Cherki, A. Khabbazi, B. Remy, and D. Baillis, "Granular cork content dependence of thermal diffusivity, thermal conductivity and heat capacity of the composite material / Granular cork bound with plaster," in *Energy Procedia*, Elsevier Ltd, 2013, pp. 83–92. doi: 10.1016/j.egypro.2013.11.008.
- [42] F. Hadji, N. Ihaddadene, R. Ihaddadene, A. Betga, A. Charick, and P. O. Logerais, "Thermal conductivity of two kinds of earthen building materials formerly used in Algeria," *Journal of Building Engineering*, vol. 32, Nov. 2020, doi: 10.1016/j.jobe.2020.101823.
- [43] Y. Hamidi, M. Malha, and A. Bah, "Analysis of the thermal behavior of hollow bricks walls filled with PCM: Effect of PCM location," *Energy Reports*, vol. 7, pp. 105–115, Nov. 2021, doi: 10.1016/j.egyr.2021.08.108.